

## Planets of $\beta$ Pictoris revisited

F. Freistetter, A. V. Krivov, and T. Löhne

Astrophysikalisches Institut, Friedrich-Schiller-Universität Jena, Schillergässchen 2-3, 07745 Jena, Germany  
e-mail: florian@astro.uni-jena.de

Received 14 November 2006 / Accepted 17 January 2007

### ABSTRACT

Observations have revealed a large variety of structures (global asymmetries, warps, belts, rings) and dynamical phenomena (“falling-evaporating bodies” or FEBs, the “ $\beta$  Pic dust stream”) in the disk of  $\beta$  Pictoris, most of which may indicate the presence of one or more planets orbiting the star. Because planets of  $\beta$  Pic have not been detected by observations yet, we use dynamical simulations to find “numerical evidence” for a planetary system. We show that one planet at 12 AU with a mass of 2 to 5  $M_J$  and an eccentricity  $\lesssim 0.1$  can probably already account for three major features (main warp, two inner belts, FEBs) observed in the  $\beta$  Pic disk. The existence of at least two additional planets at about 25 AU and 45 AU from the star seems likely. We find rather strong upper limits of 0.6  $M_J$  and 0.2  $M_J$  on the masses of those planets. The same planets could, in principle, also account for the outer rings observed at 500–800 AU.

**Key words.** celestial mechanics – minor planets, asteroids – methods:  $N$ -body simulations – stars: individual:  $\beta$  Pictoris – planetary systems – planetary systems: protoplanetary disks

### 1. Introduction

Since the discovery of the circumstellar disk of  $\beta$  Pictoris by Smith & Terrile (1984), it became the most observed and best-studied debris disk (see Lagrange et al. 2000, and references therein). However, a long-standing question whether  $\beta$  Pic also hosts planets remains unanswered. Being an A5V star,  $\beta$  Pic is a difficult target for the radial velocity measurements: the currently achieved precision of hundreds  $m\ s^{-1}$  barely excludes the presence of a 10  $M_J$  planet at 1 AU (Galland et al. 2006). The prominent edge-on disk rules out direct imaging. Transits are not promising either because of their low probability. At the same time, there is a growing bulk of indirect evidence for the presence of planets in the system. Mouillet et al. (1997) showed that a planet with an orbital inclination of  $3^\circ$  to  $5^\circ$  and a mass ranging from 0.6  $M_J$  and 18  $M_J$  between 20 and 3 AU could be responsible for the observed warp in the disk. New HST/STIS observations of the warped disk by Heap et al. (2000) changed these estimates only slightly. Augereau et al. (2001) pointed out that the same planet could explain the butterfly asymmetry of the disk. Beust & Morbidelli (2000) found that a Jovian planet at  $\approx 10$  AU with a moderate eccentricity of  $e \approx 0.05$  can explain both the warp and the observed phenomenon of falling-evaporating bodies (FEBs). Krivov et al. (2004) argued that such a planet is needed to explain the so-called “ $\beta$  Pic dust stream” detected by meteor radar AMOR (Baggaley 2000). Finally, most recent observations revealed several belt-like structures in the inner disk (Table 1) that can be attributed to the presence of planets. This work is an attempt to constrain the parameters of suspected planets in light of these observations.

### 2. Presumed planetesimal belts

Okamoto et al. (2004) performed high-resolution spectroscopic observations in the 10- $\mu m$  band to identify concentrations of submicron-sized silicate dust at 6.4 AU, 16 AU, and 30 AU, and interpreted these by dust-replenishing planetesimal belts at those

**Table 1.** Observed belt structures in the  $\beta$  Pic system.

Label	Position	Ref.
A	$\approx 6.4$ AU	2
B	$\approx 16$ AU	1, 2, 4
C	$\approx 32$ AU	1, 2, 4
D	$\approx 52$ AU	1, 3, 4

#### References:

1 = Wahhaj et al. (2003); 2 = Okamoto et al. (2004); 3 = Telesco et al. (2005); 4 = Golimowski et al. (2006).

locations. To check this interpretation, we have made test runs of our collisional code (Krivov et al. 2006). The code enables simulations of a circumstellar disk of solids over a wide range of sizes – from planetesimals to fine dust – taking into account stellar gravity and radiation pressure, as well as destructive and cratering collisions. We took a planetesimal belt of objects with radii from  $0.15\ \mu m$  to 7 km, a total mass of  $0.3\ M_\oplus$ , semimajor axes from 6 and 7 AU, and eccentricities between 0.0 and 0.1, and evolved it to a quasi-steady state to obtain a spatial distribution of dust material sustained by the belt. We then calculated the blackbody thermal emission of that dust and took a standard line-of-sight integral to obtain a brightness profile as a function of the projected distance from the star. The mass and luminosity of  $\beta$  Pic were taken to be  $1.75\ M_\odot$  and  $8\ L_\odot$  (Criko et al. 1997). We assumed a bulk density of solids of  $2.5\ g\ cm^{-3}$ .

The results are shown in Fig. 1. The flux is dominated by the emission of grains in bound orbits, or  $\alpha$ -meteoroids. However, particles in hyperbolic orbits, or  $\beta$ -meteoroids, which are particles smaller than  $\approx 2\ \mu m$ , also make a sensible contribution. The “half-peak” brightness is about a factor of two larger than in the adjacent parts of the ring, roughly consistent with the observations (Fig. 2 of Okamoto et al. 2004). A more accurate comparison is not possible for a large difference between the 6.4 AU SW and NE peaks and because the peak brightness depends on the assumed width of the planetesimal ring. The total

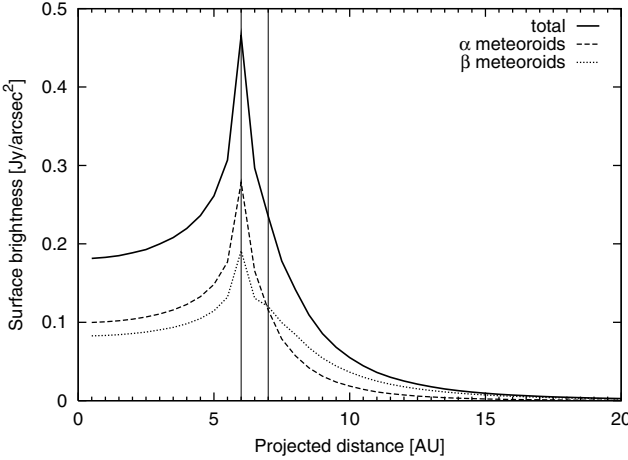


**Fig. 1.** The  $10 \mu\text{m}$  edge-on brightness of a dust “subdisk” produced by a planetesimal belt between 6 and 7 AU (as shown with vertical lines). Dashed and dotted lines: contributions from  $\alpha$ - and  $\beta$ -meteoroids, respectively; solid line: their sum.

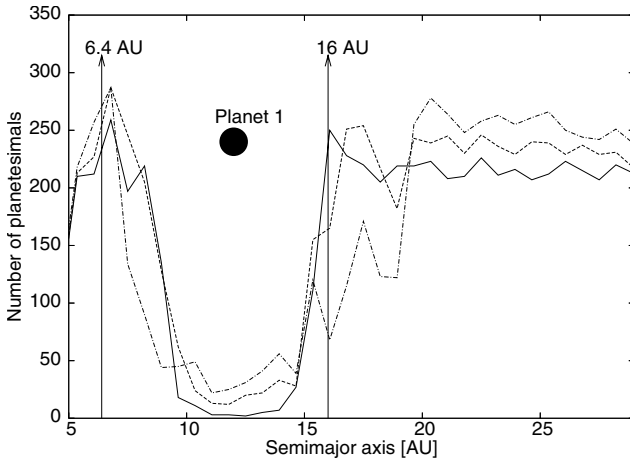


**Fig. 2.** Effect of a planet at 12 AU with  $m = 2 M_J$  on the inner part of the disk of  $\beta$  Pic (solid line:  $e = 0.01$ ; dashed line:  $e = 0.1$ ; dashed-dotted line:  $e = 0.2$ ).

mass of the planetesimal belt of  $0.3 M_\oplus$ , comparable to that of the Kuiper belt in the solar system, leads to the peak brightness  $\sim 0.3 \text{ Jy arcsec}^{-2}$ , which is close to the observed values (Okamoto et al. 2004). Therefore, we can conclude that the observed brightness peak at 6.4 AU can indeed be attributed to an invisible planetesimal belt at approximately the same location.

The results for the outer belts look similar and therefore are not shown here. Furthermore, our collisional modeling implies that, with a reasonable accuracy, possible interaction between the belts can be neglected, and that they can be treated separately.

### 3. Presumed planets

#### 3.1. Numerical model of the planetesimal disk

Numerical simulations of the motion of planetesimals were carried out with the *mercury6* integration package by Chambers (1999). The planetesimal disk was modeled by a set of massless particles, initially distributed in equidistant, circular, and plain orbits around the star, in which we placed one or more planets. Since we want to focus our study on the inner part of the disk, the orbits of particles ranged from 1 AU to 70 AU with a step size of 0.1 AU. All particles that were in Trojan-type

**Table 2.** Parameters for the proposed  $\beta$  Pic planetary system.

Planet	$m [M_J]$	$a [\text{AU}]$	$e$
1	$2.0^{+3}_{-0.5}$	$12 \pm 0.5$	$0.01^{+0.1}_{-0.01}$
2	$0.5 \pm 0.1$	$25 \pm 1$	$0.01^{+0.05}_{-0.01}$
3	$0.1^{+0.1}_{-0.03}$	$44 \pm 1$	$0.01^{+0.05}_{-0.01}$

motion with one of the planets were removed. Altogether, we performed about 100 different simulations and in each run the disk contained 20 730 particles. The integration interval was set to 12 Myr in accordance with the supposed age of the system (Zuckerman et al. 2001; Ortega et al. 2002).

#### 3.2. One planet

The first simulations were carried out with one planetary perturber. Okamoto et al. (2004) suggested that the borders of the belt at 6.4 AU are created by resonances with a planet at 12 AU, similar to the main belt in our solar system, which is confined by a 1:2 and 1:4 mean-motion resonance (MMR) with Jupiter. Thus we adopted  $a = 12 \text{ AU}$ . Mouillet et al. (1997) give a possible range for the inclination of a planet between  $3^\circ$  and  $5^\circ$  so that we chose  $i = 4^\circ$ . Three different values of the eccentricity were tested:  $e = 0.01$ ,  $e = 0.1$ , and  $e = 0.2$ . We tried the planet with several masses between 2 and  $5 M_J$ , the values that roughly bracket the range suggested to explain the warp (see Table 4 of Heap et al. 2000).

The simulation results are shown in Fig. 2. Note that this and other plots are meant to show the *positions* of belts and gaps only; to determine their strength one would need to convolve the distributions with the assumed radial density profile of the disk. The planet with  $m = 2 M_J$  opens a gap in the disk and causes a peak at 6.4 AU and a smaller peak close to 16 AU, corresponding to the A- and B-belts. The eccentricity has no influence on the peak at 6.4 AU, but the peak at 16 AU shifts outwards to  $\approx 20 \text{ AU}$  for  $e = 0.2$ . For the planet with  $m = 5 M_J$ , the peak at 6.4 AU is also present, but the second peak is at about 20 AU rather than 16 AU for all three values of eccentricity. The error bars for the estimated parameters of this planet are listed in Table 2. The limits were determined by changing the semimajor axis, eccentricity, and mass, and by checking whether the resulting peaks in the distribution of test particles still satisfy the reported observations. To avoid possible confusion in interpreting the uncertainties of semimajor axes of the proposed planets, we note that we assumed the positions of the peaks found by Okamoto et al. (2004) to be exact and give the estimated intrinsic error of *our* simulations in Table 2 and other places in the paper. However, Okamoto et al. (2004) have sampled the disk with a step of 3.2 AU, performing their measurements at discrete distances from the star of 3.2 AU, 6.4 AU, 9.5 AU, and so on. Therefore, the actual uncertainty of the semimajor axes of the predicted planets is determined by the uncertainty of the peak locations,  $\approx 2$  to 3 AU.

Although we propose that a second planet around  $\beta$  Pic makes the peak near 16 AU more prominent (see Sect. 3.3), this planet alone could already produce a notable peak. There is an analogy with the *Hilda* group of asteroids in our solar system that move near the 2:3 resonance with Jupiter and *Plutinos* in 3:2 MMR with Neptune (see, e.g., Morbidelli 2002). In our case, the 3:2 MMR with the planet at 12 AU is located at  $\sim 15.7 \text{ AU}$ . Many planetesimals in this region are resonant-protected from close encounters with the planet and form a peak with respect

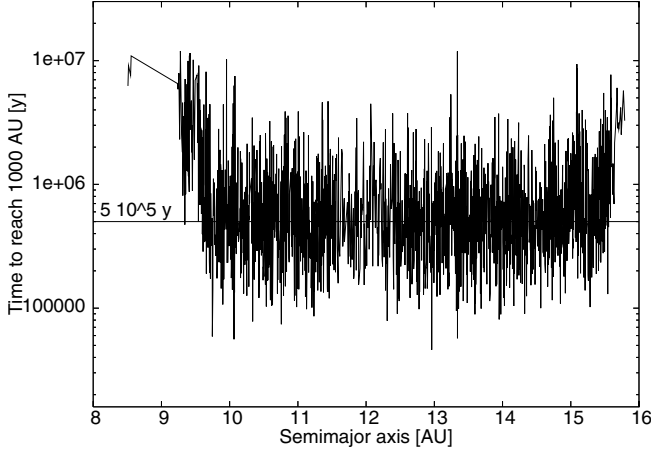


**Fig. 3.** Time needed to reach 1000 AU by the scattered particles.

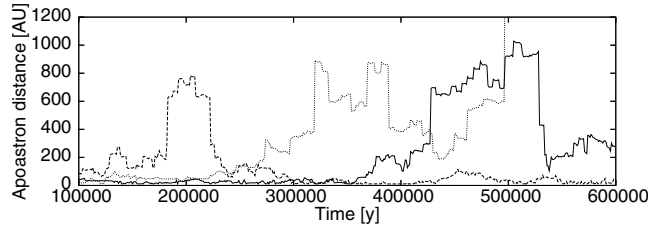


**Fig. 4.** Evolution of the apastron distance of three scattered particles.

to the non-resonant background population. Similarly, the inner peak at 6.4 AU is strongly “supported” by the 2:5 MMR in much the same way as the *Koronis* asteroid family by its 2:5 MMR with Jupiter.

The particles originally placed near the planet were scattered out of their position; some of them were thrown out of the system. Figure 3 shows the time such a particle needs to reach a distance of  $10^3$  AU. The majority need  $\sim 0.5$  Myr to reach this distance, and thus they might form some observable features in the outer parts of disk, for instance the rings observed at 500–800 AU (Kalas et al. 2001). Discrete rings may be a result of the ejection of several large planetesimals. Figure 4 shows, for three of the particles, how close encounters with the planet at 12 AU can successively change the apastron distance until it lies in the outer part of the disk.

Beust & Morbidelli (2000) analyzed the mechanisms proposed to explain the observed phenomenon of falling-evaporating bodies (FEBs). All of these – close encounters (Beust et al. 1991), the Kozai mechanism (Bailey et al. 1992), and trapping in MMRs (Beust & Morbidelli 1996) – involve the presence of at least one large planet. They showed that a planet with  $\approx 2 M_J$  at  $\approx 10$  AU with a low eccentricity can account for the detected infall of small bodies onto the star. Furthermore, they noticed that the parameters of the planet lie well inside the limits given by Mouillet et al. (1997) for a planet that can cause the observed warp. Because these parameters are close to those we found above, we can conclude that a single planet with a mass of  $m \approx 2 M_J$  at 12 AU,  $e \lesssim 0.1$  and  $i \approx 4^\circ$  can probably account for three of the major dynamical phenomena observed in the disk of  $\beta$  Pic: the warp, the A- and B-belts, and the FEBs.

### 3.3. Two and three planets

The second planet can be invoked to account for the peak around 32 AU (C-belt) that could not be created by the planet at 12 AU.

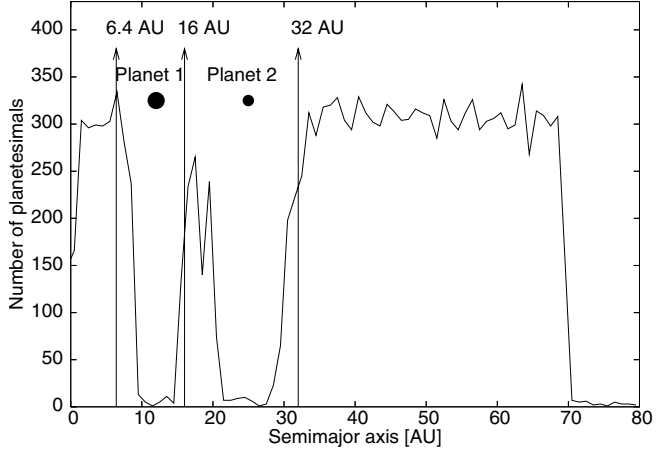


**Fig. 5.** Influence of two planets at 12 and 25 AU with  $m = 2 M_J$  and  $m = 0.5 M_J$  (both with  $e = 0.01$ ) on the disk.

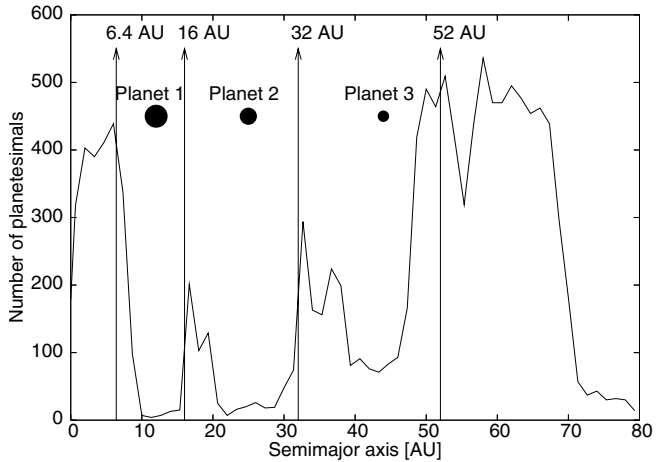


**Fig. 6.** Effect of three planets at 12, 25, and 44 AU with  $m = 2 M_J$ ,  $0.5 M_J$ , and  $0.1 M_J$  (all with  $e = 0.01$ ) on the disk.

If we follow the same strategy as for the first planet, we find that the best fit is a planet with  $m = 0.5 M_J$  at  $a = 25$  AU and  $e = 0.01$  that clears a gap and causes a new peak at 32 AU. The distribution of particles in the two-planet case is shown in Fig. 5.

Similarly, a third planet is needed to explain the peak around 52 AU (D-belt). The best fit is with  $m = 0.1 M_J$  at 44 AU. Figure 6 shows the results of our simulations with three planets. The D-belt is now created, and the peak at 32 AU became more prominent because it is now bordered by a planet on both sides. Also, the peaks at 6.4 and 16 AU are still present. It is important to mention that a more massive second planet, with a mass larger than  $\approx 0.6 M_J$ , can be excluded because it would destroy the belts. The same applies to the third planet, which cannot be more massive than  $\approx 0.2 M_J$ . Table 2 summarizes the best-fit parameters of all three planets and their error bars.

## 4. $\beta$ Pic – a resonant system?

The orbital periods of the proposed three planets are close to rational commensurabilities. Namely, the periods of planet 2 and planet 1 are nearly in a 3:1 ratio; those of planet 3 and planet 1 are close to a 7:1 ratio; and planet 3 and planet 2 are near a 7:3 commensurability. Planets in some of the extrasolar planetary systems discovered so far are known to be locked in mean-motion resonances (e.g., GJ876 or 55 Cnc). To see if the possible

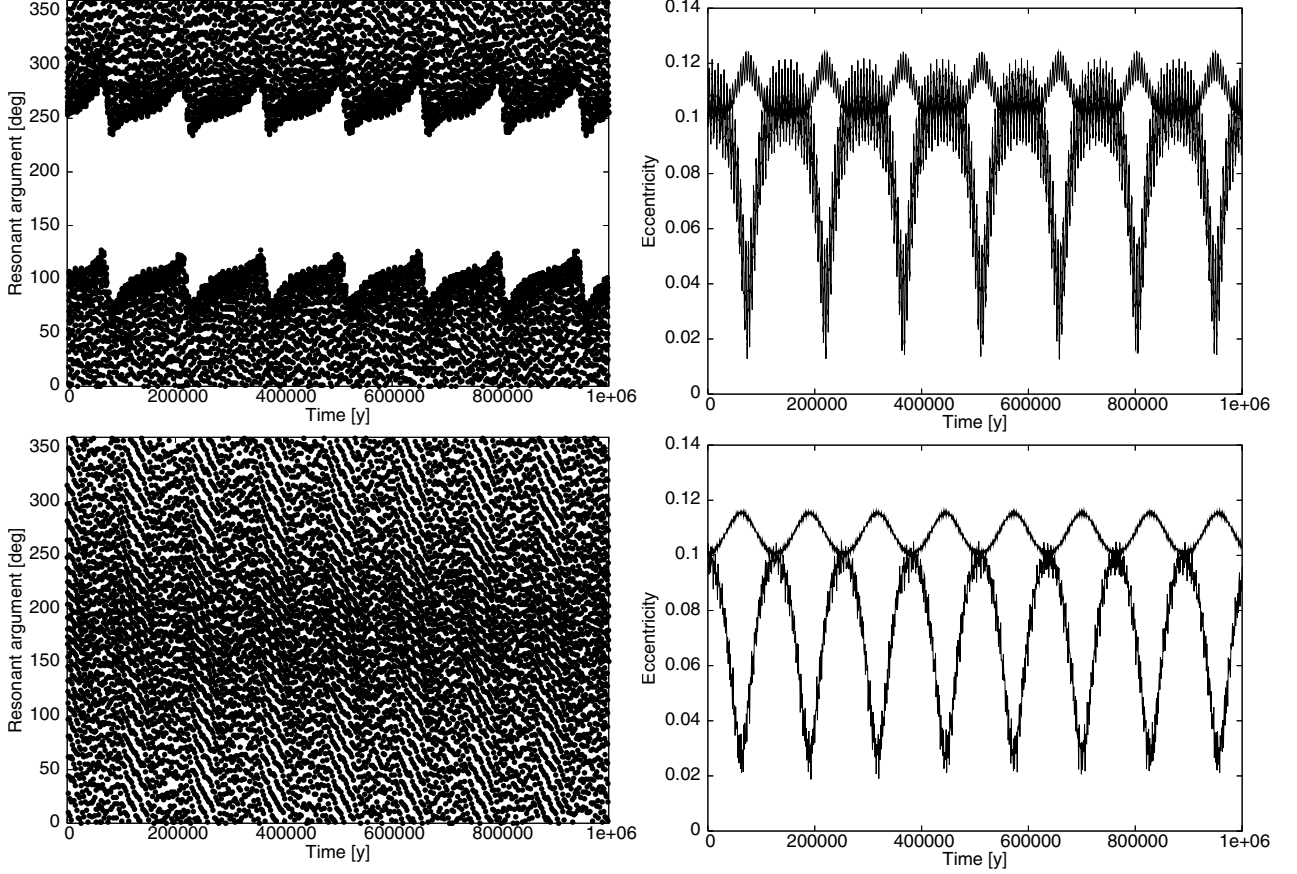


**Fig. 7.** Resonant angle  $\theta$  for the 3:1 resonance of planet 1 and planet 2 (*left*) and evolution of the eccentricities (*right*). *Top:* the case where planet 2 is located at the exact position of the resonance. *Bottom:* planet 2 is shifted by 0.1 AU inwards. Both planets have an initial eccentricity of 0.1 and an inclination of  $4^\circ$ .

planets of  $\beta$  Pic really show resonant motion, we have chosen the strongest of the three resonances mentioned above, the 3:1 MMR between the two inner planets, and calculated the resonant angle (Ji et al. 2003)

$$\theta = \lambda_1 - 3\lambda_2 + (\tilde{\omega}_1 + \tilde{\omega}_2), \quad (1)$$

where  $\lambda_i$  and  $\tilde{\omega}_i$  are the mean longitude and the longitude of periastron of the  $i$ th planet.

Figure 7 (top) shows the case where planet 2 is located at the exact position of the resonance ( $a_1 = 12.00$  AU and  $a_2 = 24.96$  AU); both planets have an initial eccentricity of 0.1. Other parameters are the same as in the simulations described in Sect. 3.3. The resonant angle librates around  $0^\circ$ , indicating the resonant locking. However, the eccentricities are not strongly affected by the resonance, which seems to be a protective one, as it is the case for GJ876 and 55 Cnc. That the effect is weak is not surprising: the resonance is rather shallow (as seen from a rather large libration amplitude), which, in turn, traces back to moderate masses of both planets and a large separation between their orbits.

We have found that a decrease in the semimajor axis of the second planet by  $\approx 0.1$  AU or an increase by  $\approx 0.2$  AU is enough to transfer  $\theta$  from libration to a circulation mode (Fig. 7, bottom). This value can be compared to analytic estimates of the resonance width. The semimajor axis of a body locked in a

resonance oscillates between  $a - \Delta a_{\max}$  and  $a + \Delta a_{\max}$ , where the libration amplitude is given by (Murray & Dermott 1999)

$$\Delta a_{\max} = a_2 \left[ \frac{16}{3} \frac{m_1}{m_*} \left( \frac{p}{p+q} \right)^{\frac{2}{3}} f_d e_2 \right]^{\frac{1}{2}} \quad (2)$$

with  $f_d = 0.5988$  for the  $(p+q):p = 3:1$  outer resonance. Assuming  $e_2 = 0.1$ , this leads to

$$\Delta a_{\max} \approx 0.3 \text{ AU}, \quad (3)$$

which is close to the value we found empirically. Thus the resonance width is smaller than the uncertainties in the semimajor axes of the planets ( $\Delta a \sim 1$  AU for our fits;  $\Delta a \sim 3$  AU for the original observations of Okamoto et al. 2004).

The eccentricity plays an important role as well. Our best fits for the three planets imply small initial eccentricities ( $e \sim 0.01$ ). With these small values, the resonant argument in our simulations was always circulating rather than librating. Libration of the resonant angle was observed, starting from  $e \gtrsim 0.07$ . The fact that the resonance gets thinner at low eccentricities is also seen from Eq. (2):  $\Delta a_{\max} \propto \sqrt{e_2}$ . Since the uncertainties of the derived semimajor axes are much larger than the precision required to distinguish resonant from non-resonant configurations, we cannot conclude whether the possible  $\beta$  Pic system is a resonant one or not. As mentioned above, some exoplanetary systems are known to be resonant. It is possible that a planetary system emerges as a resonant system – for instance, as a result of differential migration in a gaseous disk (e.g., Ferraz-Mello et al. 2005; Kley et al. 2005). Alternatively, the  $\beta$  Pic system

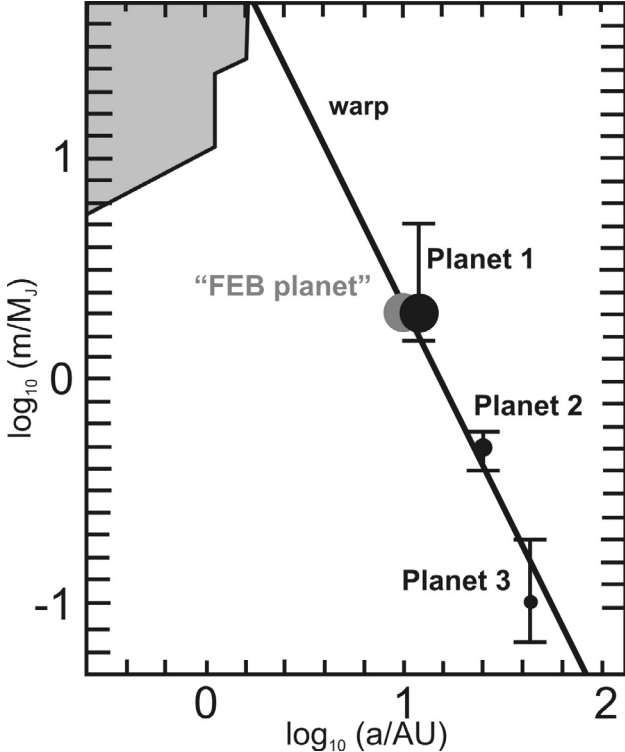


**Fig. 8.**  $\log a$ - $\log m$  phase space for alleged  $\beta$  Pic planet(s). The regions where radial velocity studies exclude a planet are shown in grey (Galland et al. 2006). Line: a planet that could cause the observed warp (Mouillet et al. 1997). Grey circle: the “FEB-planet” of Beust & Morbidelli (2000). The positions of three planets suggested by this study are shown with black circles with vertical error bars reflecting the uncertainty in the planet masses. Horizontal error bars would be indistinguishably small and therefore are not shown.

could resemble the Jupiter-Saturn configuration in our Solar System. Here the two planets are close to, but not locked in, a 5:2 resonance.

## 5. Conclusions

We have used numerical simulations to investigate the effect of one or more planets on the disk of  $\beta$  Pic. The goal was to find a minimum set of planetary perturbers that could be responsible for as many features/phenomena observed in the disk as possible. One important result is that one planet at  $\approx 12$  AU with a mass of  $m \approx 2 M_J$  and an eccentricity of  $e \lesssim 0.1$  is already able to cause three major known features: (i) two of the four belt-like structures listed in Table 1; (ii) the parameters of the planet, which lie well inside the limits given by Mouillet et al. (1997) for a planet responsible to the warp; and (iii) that this planet is similar to the one proposed by Beust & Morbidelli (2000) to explain the FEB phenomenon ( $a \approx 10$  AU,  $m = 2 M_J$ , low  $e$ ), so that the two can be considered identical. Another result is that two additional, more distant planets would naturally further explain planetesimal belts suggested by some observations. We

find rather strong upper limits on the masses of those planets:  $\approx 2 M_{SATURN}$  for a second planet at 25 AU and  $\approx 4 M_{NEPTUNE}$  for a third one at 44 AU. More massive perturbers would destroy the belts. Figure 8 shows the positions of the proposed planets in the semimajor axis-mass plane. Overplotted are regions excluded by radial velocity measurements (Galland et al. 2006), as well as the phase-space locations of the warp-inducing planet and the “FEB planet”. Interestingly, all three planets are close to the “warp planet line”.

The same planet(s) could, in principle, also account for the outer rings observed at 500–800 AU from the star (Kalas et al. 2001). A few large planetesimals could have encountered one of the inner planets in the past and, perhaps after tidal disruption during these encounters, been sent by the planets into escaping orbits or those with apocenters at hundreds of AU where the rings are observed. Further work is also needed to answer the question of if the planetary system of  $\beta$  Pic is a resonant one or not. If it really exists and the planets are in a resonant configuration, this may indicate that migration played an important role in its formation.

*Acknowledgements.* We wish to thank Philippe Thébault, Jean-Charles Augereau, Doug Hamilton, Rudolf Dvorak, Sylvio Ferraz-Mello, and Elke Pilat-Lohinger for stimulating discussions and comments on the manuscript. A speedy and helpful review provided by Hervé Beust is appreciated.

## References

- Augereau, J.-C., Nelson, R. P., Lagrange, A.-M., et al. 2001, A&A, 370, 447
- Baggaley, W. J. 2000, J. Geophys. Res., 105, 10353
- Bailey, M. E., Chambers, J. E., & Hahn, G. 1992, A&A, 257
- Beust, H., & Morbidelli, A. 1996, Icarus, 120, 358
- Beust, H., & Morbidelli, A. 2000, Icarus, 143, 170
- Beust, H., Vidal-Madjar, A., & Ferlet, R. 1991, A&A, 247, 505
- Chambers, J. E. 1999, MNRAS, 304, 793
- Cribo, F., Vidal-Madjar, A., Lallement, R., Ferlet, R., & Gerbaldi, M. 1997, A&A, 320, L29
- Ferraz-Mello, S., Michtchenko, T. A., Beaugé, C., & Callegari, Jr., N. 2005, Lect. Notes Phys., 683, 219
- Galland, F., Lagrange, A.-M., Udry, S., et al. 2006, A&A, 447, 355
- Golimowski, D. A., Ardila, D. R., Krist, J. E., et al. 2006, AJ, 131, 3109
- Heap, S. R., Lindler, D. J., Lanz, T. M., et al. 2000, ApJ, 539, 435
- Ji, J., Kinoshita, H., Liu, L., & Li, G. 2003, ApJ, 585, L139
- Kalas, P., Deltorn, J.-M., & Larwood, J. 2001, ApJ, 553, 410
- Kley, W., Lee, M. H., Murray, N., & Peale, S. J. 2005, A&A, 437, 727
- Krivov, A. V., Krivova, N. A., Solanki, S. K., & Titov, V. B. 2004, A&A, 417, 341
- Krivov, A. V., Löhne, T., & Sremčević, M. 2006, A&A, 455, 509
- Lagrange, A.-M., Backman, D. E., & Artymowicz, P. 2000, in Protostars and Planets IV, ed. V. Mannings, A. P. Boss, & S. S. Russell (Tucson: University of Arizona Press), 639
- Morbidelli, A. 2002, Modern Celestial Mechanics (London – New York: Taylor & Francis)
- Mouillet, D., Larwood, J. D., Papaloizou, J. B., & Lagrange, A.-M. 1997, MNRAS, 292, 896
- Murray, C. D., & Dermott, S. F. 1999, Solar System Dynamics (Cambridge Univ. Press)
- Okamoto, Y. K., Kataza, H., Honda, M., Yamashita, T., & 6 colleagues 2004, Nature, 431, 660
- Ortega, V. G., de la Reza, R., Jilinski, E., & Bazzanella, B. 2002, ApJ, 575, L75
- Smith, B. A., & Terrile, R. I. 1984, Science, 226, 1421
- Telesco, C. M., Fisher, R. S., Wyatt, M. C., et al. 2005, Nature, 433, 133
- Wahhaj, Z., Koerner, D. W., Ressler, M. E., et al. 2003, ApJ, 584, L27
- Zuckerman, B., Song, I., Bessell, M. S., & Webb, R. A. 2001, ApJ, 562, L87